

Point-Gap Topology of Non-Hermitian Many-Body Systems

Shu HAMANAKA^{1*} · Kazuki YAMAMOTO^{1,2†} · Tsuneya YOSHIDA^{1‡}

¹Department of Physics, Kyoto University, Kyoto 606-8502, Japan

²Department of Physics, Tokyo Institute of Technology, Meguro, Tokyo 152-8551, Japan

(Received 31 August 2023 : accepted 18 September 2023)

In the non-Hermitian system, the complex-valued spectrum leads to a unique topology known as the point-gap topology. Recent studies within a single-particle picture have shown that the nontrivial point-gap topology induces the non-Hermitian skin effect (NHSE), which denotes significant dependence of the eigenstates and eigenvalues on boundary conditions. However, most of the studies focus on the noninteracting case, and little is known about the effect of interactions on the point-gap topology. In this paper, we study the one-dimensional non-Hermitian fermionic system with a complex-valued interaction. By performing the numerical diagonalization, we demonstrate that the strong interaction induces the NHSE. Moreover, we show that the many-body topological invariant takes a nonzero value corresponding to the NHSE.

Keywords: Condensed Matter Physics, Non-Hermitian Physics, Topological Phase

I. INTRODUCTION

Recently, non-Hermitian physics is attracting much attention both theoretically and experimentally [1–3]. The non-Hermiticity allows eigenvalues of the Hamiltonian to be complex, which leads to the two types of gap structures in non-Hermitian systems [1]. One is the line-gap and the other is the point-gap. Although the line-gap topology is the generalization of the Hermitian topology, the point-gap topology is unique to non-Hermitian systems [1,2]. In the single-particle picture, it has been elucidated that the nontrivial point-gap topology causes the non-Hermitian skin effect (NHSE) [4,5], which exhibits the extreme sensitivity of eigenvalues and eigenstates to boundary conditions [6]. Specifically, under open boundary conditions (OBC), an extensive number of eigenstates are localized near the boundary. The NHSE has been experimentally observed in classical and quantum systems such as mechanical metamaterials [7] and ultracold atoms [8].

Although a lot of studies have been conducted to explore non-Hermitian topological phenomena, most of them have been restricted to noninteracting cases, and several studies have focused on the NHSE in interacting systems [9–12]. As representative examples, Refs. [9] and [10] treat the Hamiltonian with asymmetric hopping, which causes the NHSE even in single-particle systems. We note that although the Liouvillian skin effect induced by on-site interactions was proposed in Ref. [13], the eigenstates and eigenvalues of the non-Hermitian effective Hamiltonian were not analyzed in detail. Thus, the possibility of the NHSE induced by onsite interactions without asymmetric hopping remains unclear.

In this paper, we investigate the effect of onsite interactions on the point-gap topology. Specifically, we find that onsite interactions induce the NHSE in one-dimensional fermionic systems. Correspondingly, we observe that the topological invariant defined under the twisted boundary condition takes a nonzero value. The findings of this study suggest the crucial importance of interactions in the non-Hermitian topology.

*Correspondence to: hamanaka.shu.45p@st.kyoto-u.ac.jp

†Correspondence to: yamamoto@phys.titech.ac.jp

‡Correspondence to: yoshida.tsuneya.2z@kyoto-u.ac.jp



II. MODEL

In this section, we provide the model, which exhibits the NHSE in interacting systems. We study a Falicov-Kimball model [14] with a complex-valued interaction. The Hamiltonian is written by $\hat{H} = \hat{H}_0 + \hat{H}_V$, where

$$\hat{H}_0 = \sum_{k \in \text{BZ}, \alpha\beta} \hat{c}_{k\alpha\uparrow}^\dagger \mathcal{H}_{\alpha\beta}(k) \hat{c}_{k\beta\uparrow}, \quad (1)$$

$$\hat{H}_V = (V - i\gamma) \sum_j \hat{n}_{jb\uparrow} \hat{n}_{jb\downarrow}. \quad (2)$$

Here, $\hat{c}_{k\alpha\sigma}^\dagger$ ($\hat{c}_{k\alpha\sigma}$) is a fermionic creation (annihilation) operator with the momentum $k = \frac{2\pi j}{L}$ ($j = 0, \dots, L-1$) in the orbital $\alpha = a, b$ with the spin $\sigma = \uparrow, \downarrow$ state. We note that V (≥ 0) reflects the repulsive interaction between atoms and γ (≥ 0) denotes the effect of dissipation. A complex-valued interaction $V - i\gamma$ can be introduced in ultracold atoms by inducing inelastic collisions of the particles [15,16]. The non-Hermitian Hamiltonian \hat{H} describes the dynamics between the quantum jumps in the quantum trajectory approach [17]. The Bloch Hamiltonian $\mathcal{H}_{\alpha\beta}(k)$ in the orbital space reads [18]

$$\mathcal{H}(k) = d_y(k)\sigma_y + d_z(k)\sigma_z, \quad (3)$$

where

$$d_y(k) = 2t - 0.5t \sin k, \quad (4a)$$

$$d_z(k) = 2t \cos k. \quad (4b)$$

Here, σ_j ($j = x, y, z$) express the Pauli matrices in the orbital space. We note that the Hamiltonian \hat{H} has no hopping term of the down-spin state. Moreover, we do not consider the interaction of the particles in the orbital a with the down-spin state. Although this model is somewhat artificial, the experimental realization of the Falicov-Kimball model in ultracold atoms is proposed in Ref. [19]. In the following, we set t as an energy unit ($t = 1$).

III. TOPOLOGICAL INVARIANT AND INVERSION SYMMETRY

In this section, we discuss how the many-body winding number has been treated in non-Hermitian interacting systems. Although the many-body winding number is

fixed to zero under the inversion symmetry [see Eq. (7)], the winding number can be finite for our model because the first term of Eq. (4a) breaks such symmetry constraints.

First of all, when we compute the topological invariant, we have to block diagonalize the Hamiltonian. The non-Hermitian Hamiltonian \hat{H} commutes with the total number operator in the up-spin state \hat{N}_\uparrow , and the local number operator in the down-spin state $\hat{n}_{jb\downarrow}$ as

$$[\hat{H}, \hat{N}_\uparrow] = [\hat{H}, \hat{n}_{jb\downarrow}] = 0. \quad (5)$$

By making use of the relation given in Eq. (5), we can obtain the block-diagonalized Hamiltonian $\hat{H}_{N_\uparrow, \{n_\downarrow\}}$ for the subspace with N_\uparrow and $\{n_\downarrow\}$. The total number of particles in the up-spin state and the configuration of the particles in the down-spin state are denoted by N_\uparrow and $\{n_\downarrow\}$ respectively. With the block-diagonalized Hamiltonian, we can compute the topological invariant in each subspace as [9–11]

$$W_{N_\uparrow, \{n_\downarrow\}}(E_{\text{ref}}) = \oint_0^{2\pi} \frac{d\theta}{2\pi i} \frac{d}{d\theta} \log \det \left[\hat{H}_{N_\uparrow, \{n_\downarrow\}}(\theta) - E_{\text{ref}} \right]. \quad (6)$$

Here, $E_{\text{ref}} \in \mathbb{C}$ is the reference energy. The non-Hermitian Hamiltonian $\hat{H}_{N_\uparrow, \{n_\downarrow\}}(\theta)$ is defined under twisted boundary conditions, which mean that the hopping term at the boundary is multiplied by $e^{\pm i\theta}$, i.e., $c_{1\alpha\sigma}^\dagger c_{L\alpha'\sigma'} e^{i\theta}$ and $c_{L\alpha\sigma}^\dagger c_{1\alpha'\sigma'} e^{-i\theta}$.

Next, we discuss the symmetry constraint on the topological invariant defined in Eq. (6). When the Hamiltonian has the inversion symmetry

$$\hat{I} \hat{H}_{N_\uparrow, \{n_\downarrow\}}(-\theta) \hat{I}^{-1} = \hat{H}_{N_\uparrow, \{n_\downarrow\}}(\theta), \quad (7)$$

the winding number $W_{N_\uparrow, \{n_\downarrow\}}(E_{\text{ref}})$ takes zero. Here, \hat{I} is the inversion operator which is unitary and acts on the creation operator as $\hat{I} \hat{c}_{ka\sigma}^\dagger \hat{I}^{-1} = \hat{c}_{-ka\sigma}^\dagger$ and $\hat{I} \hat{c}_{kb\sigma}^\dagger \hat{I}^{-1} = -\hat{c}_{-kb\sigma}^\dagger$. In the presence of the inversion symmetry, the winding number takes zero [$W_{N_\uparrow, \{n_\downarrow\}}(E_{\text{ref}}) = 0$]. This triviality can be checked by first substituting Eq. (7) into Eq. (6). Then, we obtain $W_{N_\uparrow, \{n_\downarrow\}}(E_{\text{ref}}) = -W_{N_\uparrow, \{n_\downarrow\}}(E_{\text{ref}})$, which leads to the triviality of the winding number [$W_{N_\uparrow, \{n_\downarrow\}}(E_{\text{ref}}) = 0$].

Finally, we show that the Falicov-Kimball model given in Eqs. (1) and (2) breaks the inversion symmetry even for the noninteracting case ($V = \gamma = 0$). The inversion

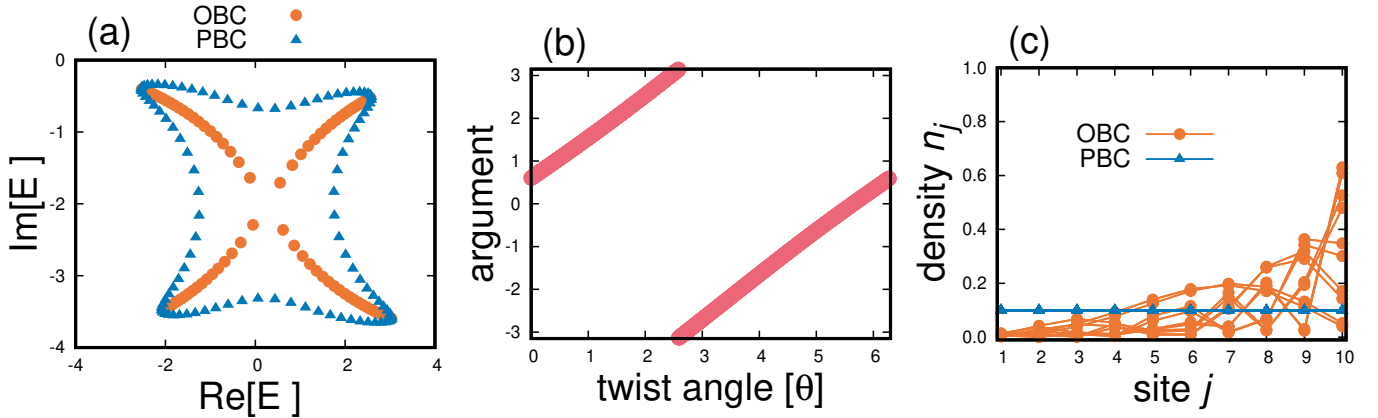


Fig. 1. (Color online) (a) Eigenvalues of the Hamiltonian under OBC (orange) and PBC (blue) for $L = 50$. (b) Argument of $\det[\hat{H}_{N_\uparrow=1, \{n_\downarrow\}}(\theta) - E_{\text{ref}}]$ for $L = 20$ and $E_{\text{ref}} = 0.0 - 1.8i$. (c) Particle density in the up-spin state under OBC (orange) and PBC (blue) for $L = 10$. In these figures, the parameters are set to be $N_\uparrow = 1$, $V = 0.5$, and $\gamma = 4.0$. The configuration of the particles in the down-spin state is set to be $\{n_\downarrow\} = \{1, \dots, 1\}$.

symmetry given in Eq. (7) in the momentum space is written by

$$\sigma_z \mathcal{H}(-k) \sigma_z^{-1} = \mathcal{H}(k). \quad (8)$$

This leads to the constraints $d_y(k) = -d_y(-k)$ and $d_z(k) = d_z(k)$. The first term $2t$ given in Eq. (4a) breaks the constraint $d_y(k) = -d_y(-k)$. Although breaking the inversion symmetry is just a necessary condition for a nonzero topological number, we demonstrate that the winding number takes a nonzero value in the following section.

IV. RESULTS

In this section, we numerically study the effects of interactions on the point-gap topology. In particular, we demonstrate that onsite interactions make the point-gap topology nontrivial and induce the NHSE. We note that when the system is noninteracting, i.e. $V = \gamma = 0$, the NHSE is absent because the Hamiltonian becomes Hermitian.

First, we show the case where the total number of particles in the up-spin state equals to one, i.e. $N_\uparrow = 1$, and then we treat the $N_\uparrow = 2$ case. Figure 1(a) shows the spectrum for $N_\uparrow = 1$ case under OBC and periodic boundary conditions (PBC). We observe that, under PBC, the spectrum forms a loop structure. Under OBC, the spectrums collapse inside the PBC spectrum

in a similar manner to the Hatano-Nelson model [20], a prototypical model exhibiting the NHSE. To verify the correspondence between nonzero topological number and the NHSE for $N_\uparrow = 1$ case, we numerically calculate the winding number given in Eq. (6). Figure 1(b) shows the argument of the determinant of $\hat{H}_{N_\uparrow=1, \{n_\downarrow\}}(\theta) - E_{\text{ref}}$ as a function of the twist angle θ . We see from Fig. 1(b) that the winding number takes one. Figure 1(c) shows the particle density under OBC and PBC. We find that although the density exhibits spatially uniform distribution under PBC, the skin modes appear near the right boundary under OBC. From the Figs. 1(a)–(c), we conclude that onsite interactions induce the NHSE for $N_\uparrow = 1$ case.

Second, we discuss another case where the total number of particles in the up-spin state equals to two. As shown in Fig. 2(a), the spectrum exhibits a complicated structure. We observe that the spectrum forms three clusters. Moreover, we find that the spectrum under OBC collapses inside the spectrum under PBC. This is the qualitatively similar behavior to that of the $N_\uparrow = 1$ case. Moreover, we see in Fig. 2(b) that the winding number takes two. The winding number taking a large value is one of the characteristic features in many-particle systems [9, 10]. We also observe that particles are localized near the right edge only under OBC [see Fig. 2(c)]. We note that contrary to $N_\uparrow = 1$ case, the Pauli exclusion principle between the particles in the up-spin state emerges for $N_\uparrow = 2$ case. The relation between the nontrivial winding number and the localization of the particles under OBC is consistent with the previous studies,

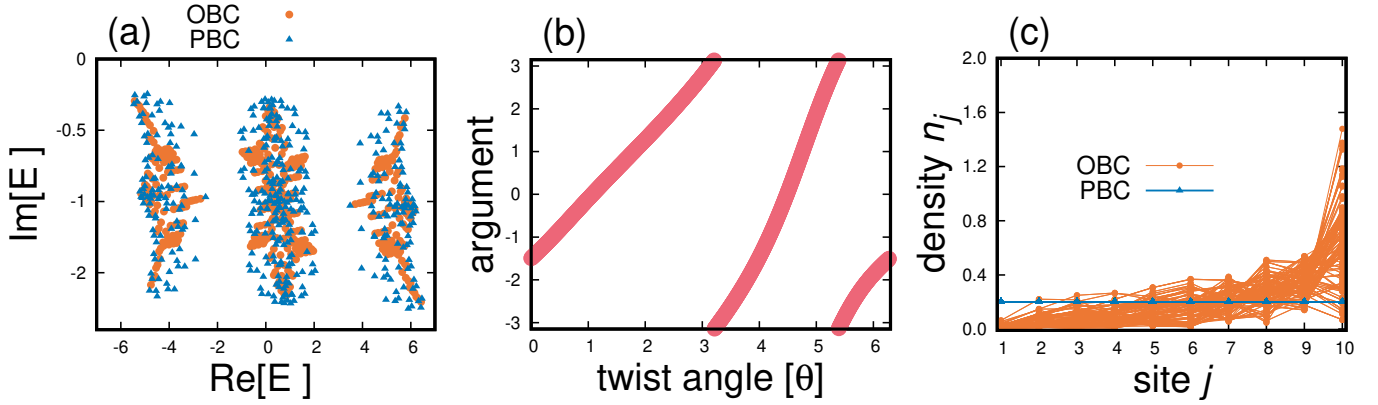


Fig. 2. (Color online) (a) Eigenvalues of the Hamiltonian under OBC (orange) and PBC (blue) for $L = 15$. (b) Argument of $\det[\hat{H}_{N_\uparrow=2, \{n_\downarrow\}}(\theta) - E_{\text{ref}}]$ for $L = 6$ and $E_{\text{ref}} = 4.9 - 0.8i$. (c) Particle density in the up-spin state under OBC (orange) and PBC (blue) for $L = 10$. In these figures, the parameters are set to be $N_\uparrow = 2$, $V = 0.5$, and $\gamma = 1.0$. The configuration of the particles in the down-spin state is set to be $\{n\}_\downarrow = \{1, \dots, 1\}$.

which have shown that the nontrivial winding number has a connection with the localization of the particle under OBC away from half-filling by analyzing the correlated Hatano-Nelson model [9, 10]. Figs. 2(a)–(c) show that even in the presence of the Pauli exclusion principle of the particles in the up-spin state, interactions induce the NHSE.

V. SUMMARY AND DISCUSSION

In this paper, we have studied the effect of interactions on the point-gap topology. Specifically, by analyzing the fermionic system with a complex-valued interaction, we have demonstrated that onsite interactions induce the NHSE. Correspondingly, we have shown that the winding number takes a nonzero value. Our results shed light on the significant role of onsite interactions in non-Hermitian many-body systems.

It is worth noting that some symmetries and two or more spatial dimensions lead to various kinds of skin effects such as symmetry-protected skin effects and higher-dimensional skin effects in noninteracting systems [4]. Analyzing the effect of interactions on these novel skin effects is left for a future study. We also note that the generalization of our results to the Lindblad master equation is interesting.

ACKNOWLEDGEMENTS

We thank Masaki Tezuka for the useful discussion. S.H. was supported by SCES2019 Fund and WISE Program. K.Y. was supported by JSPS KAKENHI Grant-in-Aid for JSPS fellows Grant No. JP20J21318 and JP23K19031. K.Y. acknowledges the support by the research grant by Yamaguchi Educational and Scholarship Foundation. This work was supported by JSPS KAKENHI Grants No. JP22H05247 and No. JP21K13850.

REFERENCES

- [1] K. Kawabata, K. Shiozaki, M. Ueda and M. Sato, *Phys. Rev. X* **9**, 041015 (2019).
- [2] Z. Gong *et al.*, *Phys. Rev. X* **8**, 031079 (2018).
- [3] F. K. Kunst, E. Edvardsson, J. C. Budich and E. J. Bergholtz, *Phys. Rev. Lett.* **121**, 026808 (2018).
- [4] N. Okuma, K. Kawabata, K. Shiozaki and M. Sato, *Phys. Rev. Lett.* **124**, 086801 (2020).
- [5] K. Zhang, Z. Yang and C. Fang, *Phys. Rev. Lett.* **125**, 126402 (2020).
- [6] S. Yao and Z. Wang, *Phys. Rev. Lett.* **121**, 086803 (2018).
- [7] A. Ghatak, M. Brandenbourger, J. van Wezel and C. Coulais, *Proc. Natl. Acad. Sci.* **117**, 29561 (2018).
- [8] L. Qian *et al.*, *Phys. Rev. Lett.* **129**, 070401 (2022).
- [9] K. Kawabata, K. Shiozaki and S. Ryu, *Phys. Rev. B* **105**, 165137 (2022).

- [10] S.-B. Zhang *et al.*, [Phys. Rev. B **106**, L121102 \(2022\)](#).
- [11] W. N. Faugno and T. Ozawa, [Phys. Rev. Lett. **129**, 180401 \(2022\)](#).
- [12] L. Mao, Y. Hao and L. Pan, [Phys. Rev. A **107**, 043315 \(2023\)](#).
- [13] S. Hamanaka, K. Yamamoto and T. Yoshida, [Phys. Rev. B **108**, 155114 \(2023\)](#).
- [14] L. M. Falicov and J. C. Kimball, [Phys. Rev. Lett. **22**, 997 \(1969\)](#).
- [15] K. Yamamoto *et al.*, [Phys. Rev. Lett. **123**, 123601 \(2019\)](#).
- [16] N. Syassen *et al.*, [Science **320**, 1329 \(2008\)](#).
- [17] A. J. Daley, [Adv. Phys. **63**, 77 \(2014\)](#).
- [18] T. Yoshida, [Phys. Rev. B **103**, 125145 \(2021\)](#).
- [19] D. Semmler, K. Byczuk and W. Hofstetter, [Phys. Rev. B **81**, 115111 \(2010\)](#).
- [20] N. Hatano and D. R. Nelson, [Phys. Rev. Lett. **77**, 570 \(1996\)](#).